Genotyping structural variation in variation graphs with the vg toolkit

This manuscript (*permalink*) *was automatically generated from jmonlong/manu-vgsv@fddfb30 on February 25, 2019.*

Authors

Ⓘ Glenn Hickey[1,☯], Ⓘ David Heller[1,☯], Ⓘ Jean Monlong[1,☯], Ⓘ Benedict Paten[1,†]

☯ — These authors contributed equally to this work

† — To whom correspondence should be addressed: bpaten@ucsc.edu

1. UC Santa Cruz Genomics Institute, University of California, Santa Cruz, California, USA

Abstract

Introduction

Structural variation (SV) represents genomic mutation involving 50 bp or more and can take several forms, such as for example deletions, insertions, inversions, or translocations. Although whole-genome sequencing (WGS) made it possible to assess virtually any type of structural variation, many challenges remain. In particular, SV-supporting reads are difficult to map to reference genomes. Multi-mapping, caused by widespread repeated sequences in the genome, is another issue because it often resembles SV-supporting signal. As a result, many SV detection algorithms have been developed and multiple methods must usually be combined to minimize false positives. Several large-scale projects used this ensemble approach, cataloging tens of thousands of SV in humans[1,2]. SV detection from short-read sequencing remains laborious and of lower accuracy, explaining why these variants and their impact have been under-studied as compared to single-nucleotide variants (SNVs) and small insertions/deletions (indels).

Over the last few years, exciting developments in sequencing technologies and library preparation made it possible to produce long reads or retrieve long-range information over kilobases of sequence. These approaches are maturing to the point were it is feasible to analyze the human genome. This multi-kbp information is particularly useful for SV detection and de novo assembly. In the last few years, several studies using long-read or linked-read sequencing have produced large catalogs of structural variation, the majority of which were novel and sequence-resolved[3,4,5,6,7]. These technologies are also enabling high-quality de novo genome assemblies to be produced[3, 8], as well as large blocks of haplotype-resolved sequences[9]. These technological advances promise to expand the amount of known genomic variation in humans in the near future.

In parallel, the reference genome is evolving from a linear reference to a graph-based reference that contains known genomic variation[10,11,12]. By having variants in the graph, mapping rates are increased and variants are more uniformly covered, including indels and variants in complex regions[11]. Both the mapping and variant calling become variant-aware and benefit in term of accuracy and sensitivity. In addition, different variant types are called simultaneously by a unified framework. Graphs have also been used locally, i.e. to call variants at the region level. GraphTyper[13] and BayesTyper[14] both construct variation graphs of small regions and use them for variant genotyping. Here again, the graph-approach showed clear advantages over standard approaches that use the linear reference. Other SV genotyping approaches compare read mapping in the reference genome and a sequence modified with the SV. For example SMRT-SV was designed to genotype SVs identified on PacBio reads[4], SVTyper uses paired-end mapping and split-read mapping information[15], and Delly provides a genotyping feature in addition to its discovery mode[16].

Results

Structural variation in vg

In addition to SNV and short indels, vg can handle large deletions and insertions (and inversion?) (Figure 1). As a proof-of-concept we simulated genomes and SVs with a size distribution matching real SVs[17]. Some errors were added at the breakpoints to investigate their effect on genotyping. In all simulations, vg performed as well or better than SVtyper[15] and Delly[16] (Figure 2). Overall, vg was more robust to errors around the breakpoints. For insertions, vg performed almost as well as in the presence of errors in contrast to Delly and BayesTyper whose performance dropped significantly. For deletions, the F1 dropped for all methods but remained high for vg and SVtyper.
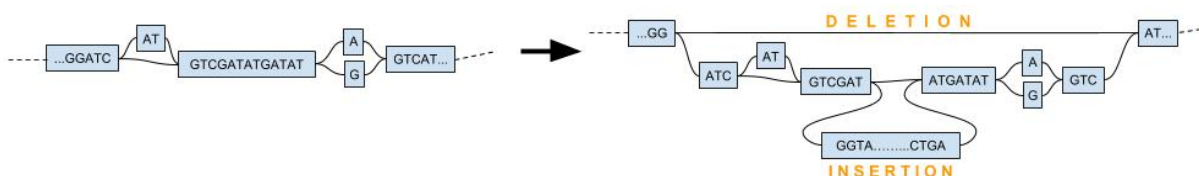

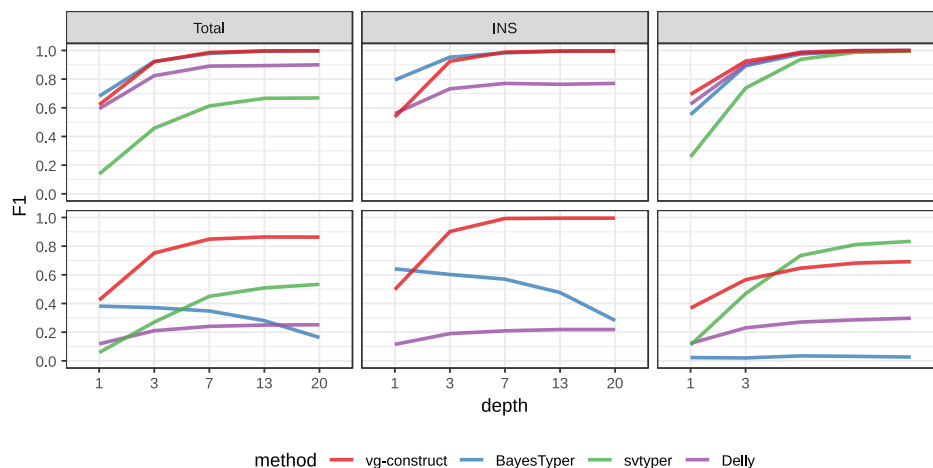Figure 1: **Large deletions and insertions in variation graphs**

Figure 2: **Simulation experiment**. For each experiment (method, depth and input VCF with/without erros), the deciles of the call qualities were used as threshold and the maximum F1 is reported on the y-axis.

HGSVC

Chaisson et al.[17] provide a high-quality SV catalog of three samples, obtained using a consensus from different sequencing, phasing and variant caling technologies.

(Whole-genome) Simulation

The phasing information in the HGSVC VCF was used to extract two haplotypes for sample HG00514, and 30X pairend-end reads were simulated using vg sim. The reads were used to call VCFs then compared back to the original HGSVC calls (Figure 3 and Table 1).

When restricting the comparisons to regions not identified as tandem repeats or segmental duplications in the Genome Browser (Table 2).
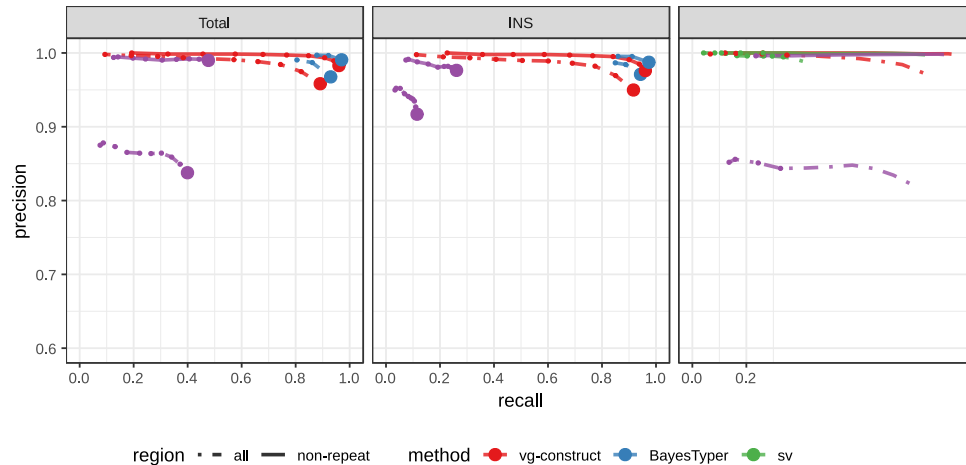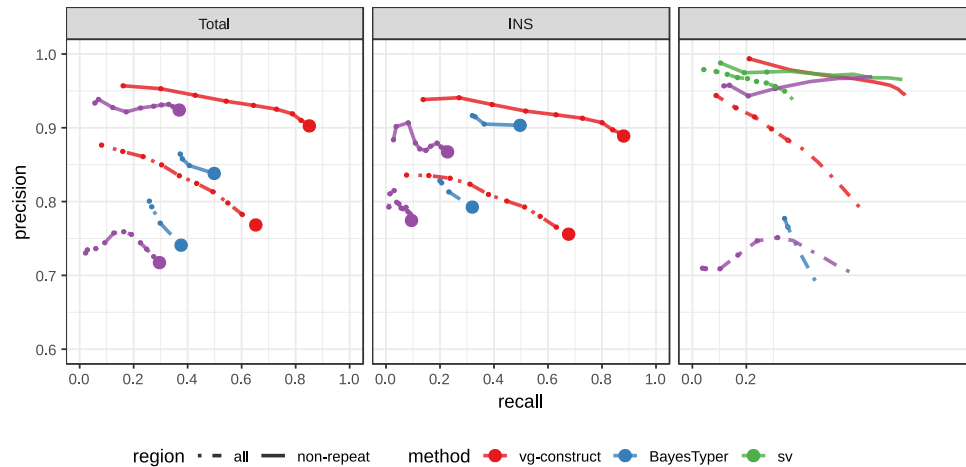

Figure 3: **HGSVC simulated reads**.

Figure 4: **HGSVC real reads**.

(Whole-genome) Real reads

Figure 4. Tables 3 and 4 for results over the genome or when restricting the comparisons to regions not identified as tandem repeats or segmental duplications in the Genome Browser.

The input SVs could also be derived from short-reads. For example, SVs were first discovered by Manta(REF) from Illumina reads and then genotyped. For BayesTyper, the precision drops for insertions while the recall increases for deletions (Figure 9).

Genotyping SV using vg and de novo assemblies

We investigated whether genome graphs derived from genome-genome alignments yield advantages for SV genotyping. To this end, we analyzed public sequencing datasets for 12 yeast strains from two clades (S. cerevisiae and S. paradoxus) [18]. From these datasets, we generated two different types of genome graphs. The first graph type (in the following called *construct graph*) was created from a linear reference genome of the S.c. S288C strain and a set of SVs relative to this reference strain in VCF format. We compiled the SV set using the output of three methods for SV detection from genome assemblies: Assemblytics [19], AsmVar [20] and paftools [21]. All three methods were run to detect SVs between the reference strain S.c. S288C and each of the other 11 strains. Merging the results from the three methods and the 11 strains provided us with a high-sensitivity set of SVs occuring in the two yeast clades. We used this set to construct the *construct graph*. The second graph (in the following called *cactus graph*) was derived from a multiple genome alignment of all 12 strains using our Cactus tool [22]. While the *construct graph* is still mainly linear and highly dependent on the reference genome, the cactus graph is completely unbiased in that regard.
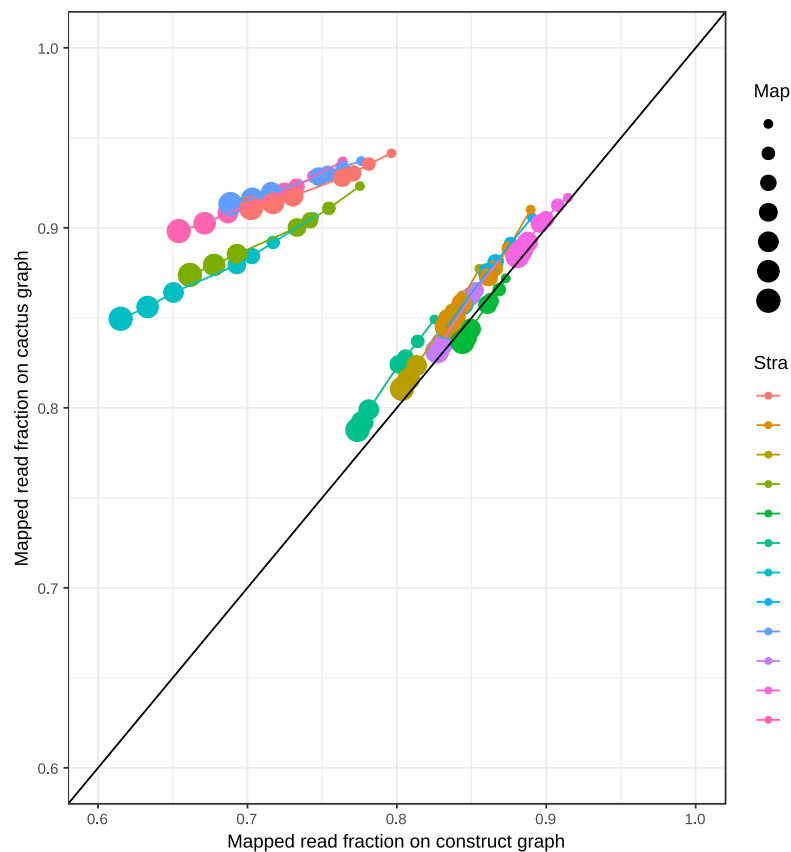

Figure 5: **Mapping quality comparison.** The fraction of reads mapped (with different mapping quality thresholds) to the cactus graph (y-axis) and the construct graph (x-axis) are compared
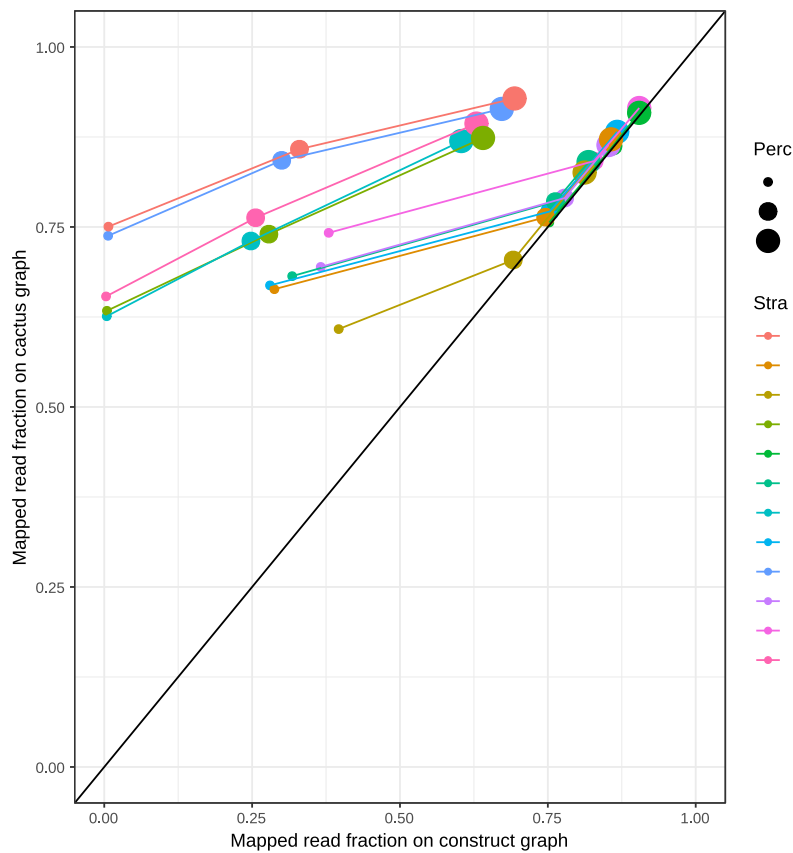
Figure 6: **Mapping identity comparison.** The fraction of reads mapped (with different percent identity thresholds) to the cactus graph (y-axis) and the construct graph (x-axis) are compared

In a first step, we tested our hypothesis that the *cactus graph* has higher mappability due to its better representation of sequence diversity among the yeast strains. When mapping short Illumina reads from the 12 strains to both graphs, we indeed observed a higher fraction of reads mapped to the *cactus graph* than to the *construct graph* (see Fig. 5). Only for the reference strain S.c. S288C, both graphs exhibited similar mappability. This suggests that not the higher sequence content in the *cactus graph* alone (XX Mb compared to XX Mb in the *construct graph*) drives the improvement in mappability. Instead, our measurements suggest that genetic distance to the reference strain increases the advantage of the *cactus graph* over the *construct graph*. Consequently. the gap is largest for strains in the S. paradoxus clade and smaller for reads from strains in the S. cerevisiae clade.
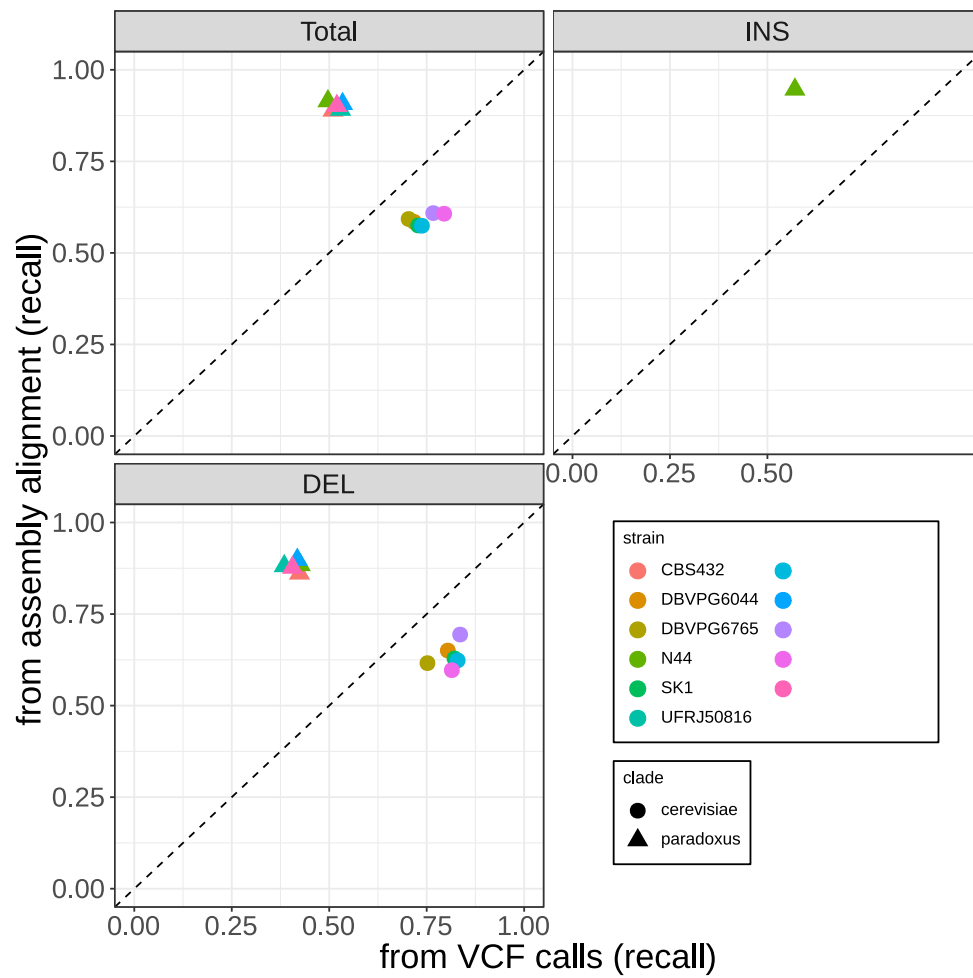
Figure 7: **SV genotyping comparison.** SV genotype recall from the *cactus graph* (y-axis) and *construct graph* (x-axis) are compared. Colors and shapes represent the 12 strains and two clades, respectively
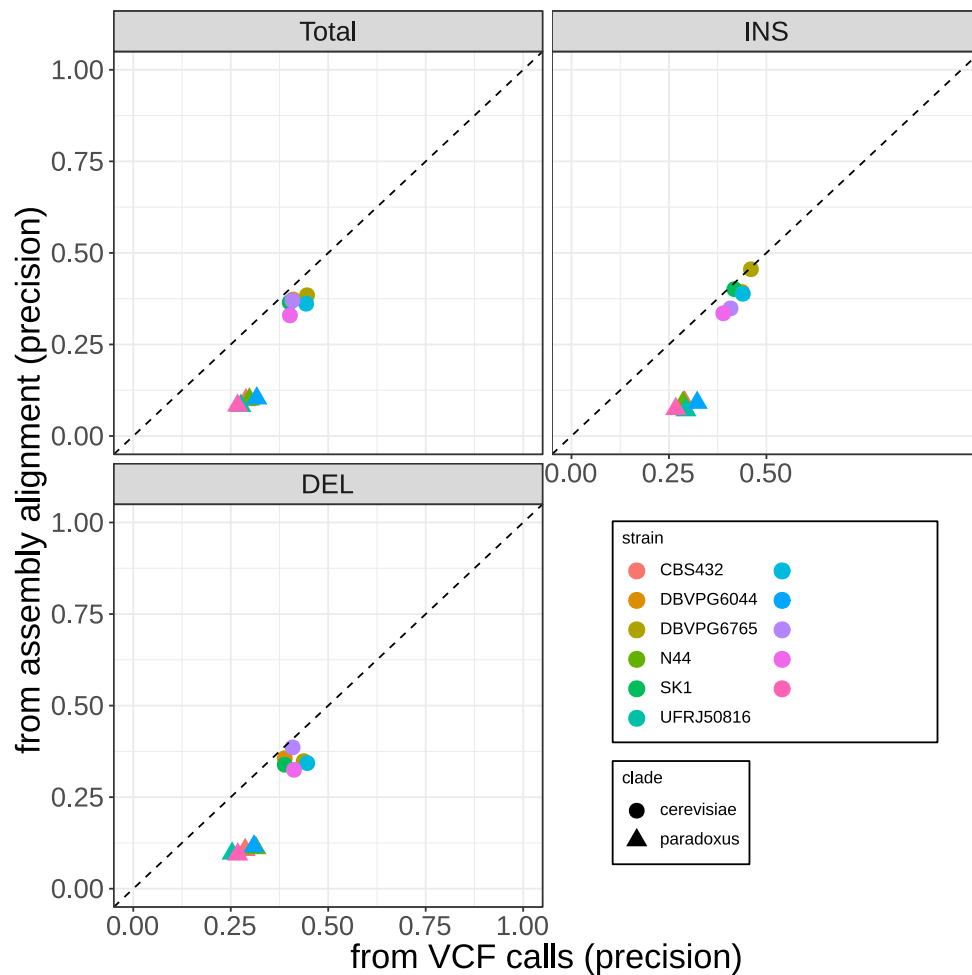
Figure 8: **SV genotyping comparison.** SV genotype precision from the *cactus graph* (y-axis) and *construct graph* (x-axis) are compared. Colors and shapes represent the 12 strains and two clades, respectively

Next, we compared the SV genotype performance of both graphs. To facilitate a fair evaluation of genotype performance, we combined all SVs that were detected by at least two of the three SV callers (Assemblytics, AsmVar and paftools) into a truth set. This truth set is a subset of the SV set used for construction of the *construct graph* which is important because only variants already present in the graph can be genotyped.

Figure 7 and 8 shows the results of our analysis. Depending on the clade, the *cactus graph* reaches either a substantially higher SV genotyping recall than the *construct graph* (S. paradoxus) or a substantially lower recall (S. cerevisiae).

Methods

Discussion

Supplementary Material

Table 1: HGSVC experiment using simulated reads.

Graph	type	TP	TP.baseline	FP	FN	precision	recall	F1
HGSVC-Construct	Total	24451	24089	3119	2617	0.8854	0.902	0.8936
	INS	14596	14264	775	1421	0.9485	0.9094	0.9285
	DEL	9855	9825	2344	1196	0.8074	0.8915	0.8474
HGSVC-1KG-Construct	Total	24172	23815	3236	2891	0.8804	0.8917	0.886
	INS	14540	14111	836	1574	0.9441	0.8996	0.9213
	DEL	9632	9704	2400	1317	0.8017	0.8805	0.8393
HGSVC-Bayestyper	Total	13895	14362	123	12344	0.9915	0.5378	0.6974
	INS	8473	8757	102	6928	0.9885	0.5583	0.7136
	DEL	5422	5605	21	5416	0.9963	0.5086	0.6734
SVPOP-Construct	Total	10548	11559	5990	15147	0.6587	0.4328	0.5224
	INS	7733	8223	2266	7462	0.784	0.5243	0.6284
	DEL	2815	3336	3724	7685	0.4725	0.3027	0.369
SVPOP-1KG-Construct	Total	10403	11369	6750	15337	0.6275	0.4257	0.5073
	INS	7497	7934	2198	7751	0.7831	0.5058	0.6146
	DEL	2906	3435	4552	7586	0.4301	0.3117	0.3615

Table 2: HGSVC experiment using simulated reads and restricting the comparisons to non-repeat regions.

Graph	type	TP	TP.baseline	FP	FN	precision	recall	F1
HGSVC-Construct	Total	5901	5822	452	253	0.928	0.9584	0.943
	INS	4026	3952	98	172	0.9758	0.9583	0.967
	DEL	1875	1870	354	81	0.8408	0.9585	0.8958
HGSVC-1KG-Construct	Total	5880	5785	486	290	0.9225	0.9523	0.9372
	INS	4024	3922	123	202	0.9696	0.951	0.9602
	DEL	1856	1863	363	88	0.8369	0.9549	0.892
HGSVC-Bayestyper	Total	3805	3863	8	2212	0.9979	0.6359	0.7768
	INS	2401	2430	6	1694	0.9975	0.5892	0.7408
	DEL	1404	1433	2	518	0.9986	0.7345	0.846
SVPOP-Construct	Total	3565	3856	390	2219	0.9081	0.6347	0.7472
	INS	3091	3246	239	878	0.9314	0.7871	0.8532
	DEL	474	610	151	1341	0.8016	0.3127	0.4499
SVPOP-1KG-Construct	Total	3574	3817	562	2258	0.8717	0.6283	0.7303
	INS	3066	3180	253	944	0.9263	0.7711	0.8416
	DEL	508	637	309	1314	0.6734	0.3265	0.4398

Table 3: HGSVC experiment using real reads.

Graph	type	TP	TP.baseline	FP	FN	precision	recall	F1
HGSVC-Construct	Total	18436	18500	6575	8206	0.7378	0.6927	0.7145
	INS	10984	10600	3542	5085	0.7495	0.6758	0.7107
	DEL	7452	7900	3033	3121	0.7226	0.7168	0.7197
HGSVC-1KG-Construct	Total	17802	17946	6221	8760	0.7426	0.672	0.7055
	INS	10647	10262	3304	5423	0.7564	0.6543	0.7017
	DEL	7155	7684	2917	3337	0.7248	0.6972	0.7107
HGSVC-Bayestyper	Total	4342	4840	1048	21866	0.822	0.1812	0.2969
	INS	1786	1883	309	13802	0.859	0.1201	0.2107
	DEL	2556	2957	739	8064	0.8001	0.2683	0.4018
SVPOP-Construct	Total	9091	9931	10235	16775	0.4925	0.3719	0.4238
	INS	6972	7420	6706	8265	0.5253	0.4731	0.4978
	DEL	2119	2511	3529	8510	0.4157	0.2278	0.2943

Table 4: HGSVC experiment using real reads and restricting the comparisons to non-repeat regions.

Graph	type	TP	TP.baseline	FP	FN	precision	recall	F1
HGSVC-Construct	Total	5197	5244	854	831	0.86	0.8632	0.8616
	INS	3708	3626	459	498	0.8876	0.8792	0.8834
	DEL	1489	1618	395	333	0.8038	0.8293	0.8164
HGSVC-1KG-Construct	Total	5103	5155	865	920	0.8563	0.8486	0.8524
	INS	3642	3555	464	569	0.8845	0.862	0.8731
	DEL	1461	1600	401	351	0.7996	0.8201	0.8097
HGSVC-Bayestyper	Total	1560	1731	274	4344	0.8633	0.2849	0.4284
	INS	883	901	69	3223	0.9289	0.2185	0.3538
	DEL	677	830	205	1121	0.8019	0.4254	0.5559
SVPOP-Construct	Total	3251	3480	941	2595	0.7872	0.5728	0.6631
	INS	2859	3009	780	1115	0.7941	0.7296	0.7605
	DEL	392	471	161	1480	0.7453	0.2414	0.3647
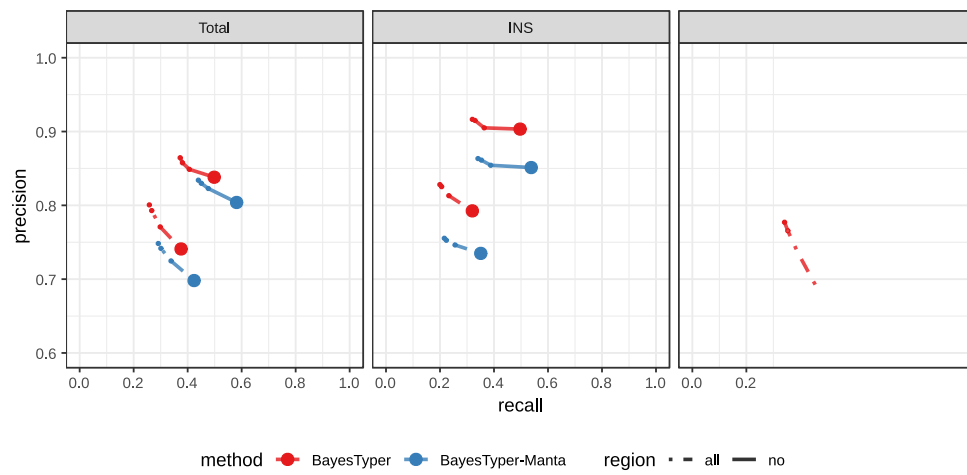
Figure 9: **HGSVC real reads**. The genotypers were run using either SVs from the HGSVC catalog (PacBio) or SVs discovered from short-reads using Manta

References

1. **An integrated map of structural variation in 2,504 human genomes**
Peter H. SudmantTobias Rausch, Eugene J. Gardner, Robert E. Handsaker, Alexej Abyzov, John Huddleston, Yan Zhang, Kai Ye, Goo Jun, … Jan O. Korbel
Nature (2015-10) https://doi.org/73c
DOI: 10.1038/nature15394 · PMID: 26432246 · PMCID: PMC4617611

2. **Whole-genome sequence variation, population structure and demographic history of the Dutch population**
Laurent C FrancioliAndroniki Menelaou, Sara L Pulit, Freerk van Dijk, Pier Francesco Palamara, Clara C Elbers, Pieter BT Neerincx, Kai Ye, Victor Guryev, … Cisca Wijmenga
Nature Genetics (2014-06-29) https://doi.org/f6bxm8
DOI: 10.1038/ng.3021 · PMID: 24974849

3. **Resolving the complexity of the human genome using single-molecule sequencing**
Mark J. P. Chaisson, John Huddleston, Megan Y. Dennis, Peter H. Sudmant, Maika Malig, Fereydoun Hormozdiari, Francesca Antonacci, Urvashi Surti, Richard Sandstrom, Matthew Boitano, … Evan E. Eichler
Nature (2014-11-10) https://doi.org/w69
DOI: 10.1038/nature13907 · PMID: 25383537 · PMCID: PMC4317254

4. **Discovery and genotyping of structural variation from long-read haploid genome sequence data**
John Huddleston, Mark J.P. Chaisson, Karyn Meltz Steinberg, Wes Warren, Kendra Hoekzema, David Gordon, Tina A. Graves-Lindsay, Katherine M. Munson, Zev N. Kronenberg, Laura Vives, … Evan E. Eichler
Genome Research (2016-11-28) https://doi.org/f9x79h
DOI: 10.1101/gr.214007.116 · PMID: 27895111 · PMCID: PMC5411763

5. **Mapping and phasing of structural variation in patient genomes using nanopore sequencing**
Mircea Cretu Stancu, Markus J. van Roosmalen, Ivo Renkens, Marleen M. Nieboer, Sjors Middelkamp, Joep de Ligt, Giulia Pregno, Daniela Giachino, Giorgia Mandrile, Jose Espejo Valle-Inclan, … Wigard P. Kloosterman
Nature Communications (2017-11-06) https://doi.org/gftpt9
DOI: 10.1038/s41467-017-01343-4 · PMID: 29109544 · PMCID: PMC5673902

6. **Genome-wide reconstruction of complex structural variants using read clouds**
Noah Spies, Ziming Weng, Alex Bishara, Jennifer McDaniel, David Catoe, Justin M Zook, Marc Salit, Robert B West, Serafim Batzoglou, Arend Sidow

Nature Methods (2017-07-17) https://doi.org/gbnhwk
DOI: 10.1038/nmeth.4366 · PMID: 28714986 · PMCID: PMC5578891

7. **Characterizing the Major Structural Variant Alleles of the Human Genome**
Peter A. Audano, Arvis Sulovari, Tina A. Graves-Lindsay, Stuart Cantsilieris, Melanie Sorensen, AnneMarie E. Welch, Max L. Dougherty, Bradley J. Nelson, Ankeeta Shah, Susan K. Dutcher, … Evan E. Eichler
Cell (2019-01) https://doi.org/gfthvz
DOI: 10.1016/j.cell.2018.12.019 · PMID: 30661756

8. **Nanopore sequencing and assembly of a human genome with ultra-long reads**
Miten Jain, Sergey Koren, Karen H Miga, Josh Quick, Arthur C Rand, Thomas A Sasani, John R Tyson, Andrew D Beggs, Alexander T Dilthey, Ian T Fiddes, … Matthew Loose
Nature Biotechnology (2018-01-29) https://doi.org/gczffw
DOI: 10.1038/nbt.4060 · PMID: 29431738 · PMCID: PMC5889714

9. **Phased diploid genome assembly with single-molecule real-time sequencing**
Chen-Shan Chin, Paul Peluso, Fritz J Sedlazeck, Maria Nattestad, Gregory T Concepcion, Alicia Clum, Christopher Dunn, Ronan O'Malley, Rosa Figueroa-Balderas, Abraham Morales-Cruz, … Michael C Schatz
Nature Methods (2016-10-17) https://doi.org/f9fv4w
DOI: 10.1038/nmeth.4035 · PMID: 27749838 · PMCID: PMC5503144

10. **Genome graphs and the evolution of genome inference**
Benedict Paten, Adam M. Novak, Jordan M. Eizenga, Erik Garrison
Genome Research (2017-03-30) https://doi.org/f95nhd
DOI: 10.1101/gr.214155.116 · PMID: 28360232 · PMCID: PMC5411762

11. **Variation graph toolkit improves read mapping by representing genetic variation in the reference**
Erik Garrison, Jouni Sirén, Adam M Novak, Glenn Hickey, Jordan M Eizenga, Eric T Dawson, William Jones, Shilpa Garg, Charles Markello, Michael F Lin, … Richard Durbin
Nature Biotechnology (2018-08-20) https://doi.org/gd2zqs
DOI: 10.1038/nbt.4227 · PMID: 30125266 · PMCID: PMC6126949

12. **Fast and accurate genomic analyses using genome graphs**
Goran Rakocevic, Vladimir Semenyuk, Wan-Ping Lee, James Spencer, John Browning, Ivan J. Johnson, Vladan Arsenijevic, Jelena Nadj, Kaushik Ghose, Maria C. Suciu, … Deniz Kural
Nature Genetics (2019-01-14) https://doi.org/gftd46
DOI: 10.1038/s41588-018-0316-4 · PMID: 30643257

13. **Graphtyper enables population-scale genotyping using pangenome graphs**
Hannes P Eggertsson, Hakon Jonsson, Snaedis Kristmundsdottir, Eirikur Hjartarson, Birte Kehr,

Gisli Masson, Florian Zink, Kristjan E Hjorleifsson, Aslaug Jonasdottir, Adalbjorg Jonasdottir, …
Bjarni V Halldorsson
Nature Genetics (2017-09-25) https://doi.org/gbx7v6
DOI: 10.1038/ng.3964 · PMID: 28945251

14. **Accurate genotyping across variant classes and lengths using variant graphs**
Jonas Andreas SibbesenLasse Maretty, Anders Krogh
Nature Genetics (2018-06-18) https://doi.org/gdndnz
DOI: 10.1038/s41588-018-0145-5 · PMID: 29915429

15. **SpeedSeq: ultra-fast personal genome analysis and interpretation**
Colby Chiang, Ryan M Layer, Gregory G Faust, Michael R Lindberg, David B Rose, Erik P
Garrison, Gabor T Marth, Aaron R Quinlan, Ira M Hall
Nature Methods (2015-08-10) https://doi.org/gcpgfh
DOI: 10.1038/nmeth.3505 · PMID: 26258291 · PMCID: PMC4589466

16. **DELLY: structural variant discovery by integrated paired-end and split-read analysis**
T. Rausch, T. Zichner, A. Schlattl, A. M. Stutz, V. Benes, J. O. Korbel
Bioinformatics (2012-09-07) https://doi.org/f38r2c
DOI: 10.1093/bioinformatics/bts378 · PMID: 22962449 · PMCID: PMC3436805

17. **Multi-platform discovery of haplotype-resolved structural variation in human genomes**
Mark J.P. Chaisson, Ashley D. Sanders, Xuefang Zhao, Ankit Malhotra, David Porubsky, Tobias
Rausch, Eugene J. Gardner, Oscar Rodriguez, Li Guo, Ryan L. Collins, … Charles Lee
Cold Spring Harbor Laboratory (2017-09-23) https://doi.org/gftxhc
DOI: 10.1101/193144

18. **Contrasting evolutionary genome dynamics between domesticated and wild yeasts**
Jia-Xing Yue, Jing Li, Louise Aigrain, Johan Hallin, Karl Persson, Karen Oliver, Anders Bergström,
Paul Coupland, Jonas Warringer, Marco Cosentino Lagomarsino, … Gianni Liti
Nature Genetics (2017-04-17) https://doi.org/f93kpp
DOI: 10.1038/ng.3847 · PMID: 28416820 · PMCID: PMC5446901

19. **Assemblytics: a web analytics tool for the detection of variants from an assembly**
Maria Nattestad, Michael C. Schatz
Bioinformatics (2016-06-17) https://doi.org/f9c485
DOI: 10.1093/bioinformatics/btw369 · PMID: 27318204 · PMCID: PMC6191160

20. **Discovery, genotyping and characterization of structural variation and novel sequence
at single nucleotide resolution from de novo genome assemblies on a population scale**
Siyang LiuShujia Huang, Junhua Rao, Weijian Ye, Anders Krogh, Jun Wang
GigaScience (2015-12) https://doi.org/f75r4n
DOI: 10.1186/s13742-015-0103-4 · PMID: 26705468 · PMCID: PMC4690232

21. **Minimap2: pairwise alignment for nucleotide sequences**

Heng Li

Bioinformatics (2018-05-10) https://doi.org/gdhbqt

DOI: 10.1093/bioinformatics/bty191 · PMID: 29750242 · PMCID: PMC6137996

22. **Cactus: Algorithms for genome multiple sequence alignment**

B. Paten, D. Earl, N. Nguyen, M. Diekhans, D. Zerbino, D. Haussler

Genome Research (2011-06-10) https://doi.org/bk4697

DOI: 10.1101/gr.123356.111 · PMID: 21665927 · PMCID: PMC3166836